CLINICAL RESEARCH

3D Printing Characteristics and Mechanical Properties of a Bio Scaffold Obtained from a Micro-CT Scan, Using the Fused Deposition Modeling Technique

Características de la impresión 3D y propiedades mecánicas de un bioandamio generado a partir de un Micro-CT Scan, utilizando la técnica de modelado por deposición fundida

Natalia González-Sánchez DDS[1]; Nicole Jensen-Líos DDS[2];
Diana Hernández-Montoya MATIE[3]; José Esteban Campos Zumbado Bach[4];
Jorge Oviedo-Quirós DDS, OMFS, MSD[5]

1. General Dentist, Private Practice, Hospital Cima, San José, Costa Rica.
https://orcid.org/0000-0001-7088-3222
2. General Dentist, Private Practice, Hospital Cima, San José, Costa Rica.
https://orcid.org/0000-0002-8157-7957
3. Vice-Rectory of Research, Kä Träre Manufacturing Laboratory, Universidad Estatal a Distancia, San José, Costa Rica. https://orcid.org/0000-0002-8219-3234
4. Vice-Rectory of Research, Kä Träre Manufacturing Laboratory, Universidad Estatal a Distancia, San José, Costa Rica. https://orcid.org/0000-0002-8941-815X
5. Cleft Lip Palate-Craniomaxillofacial Unit, National Children's Hospital "Dr. Carlos Sáenz Herrera". School of Dentistry, University of Costa Rica, San José, Costa Rica.
https://orcid.org/0000-0003-0211-5939

Correspondence to: Dr. Jorge Oviedo-Quirós - jorge.oviedo@ucr.ac.cr

ABSTRACT: The objective is to determine which biopolymer has the best 3D printing characteristics and mechanical properties for the manufacture of a bioscaffold, using the fused deposition printing technique, with models generated from an STL file obtained from a Micro-CT scan taken from a bovine iliac crest bone structure. Through an experimental exploratory study, three study groups of the analyzed biopolymers were carried out with thirteen printed structures of each one. The first is made of 100% PLA. The second, 90B, we added 1g of diatom extract, and the third, 88C, differs from the previous one in that it also contains 1g of calcium phosphate. The 39 printed structures underwent a visual inspection test, which required the fabrication of a gold standard scaffold in resin, with greater detail and similarity to the scanned bone structure. Finally, the structures were subjected to a compressive force (N) to obtain

GONZÁLEZ-SÁNCHEZ N., JENSEN-LÍOS N., HERNÁNDEZ-MONTOYA D., CAMPOS J.E., OVIEDO-QUIRÓS J., 2023: 3D Printing Characteristics and Mechanical Properties of a Bio Scaffold Obtained from a Micro-CT Scan, Using the Fused Deposition Modeling Technique.-ODOVTOS-Int. J. Dental Sc.-ODOVTOS-Int. J. Dental Sc., 25-2 (May-August): 112-122

ODOVTOS-Int. J. Dent. Sc. | No. 25-2: 112-122, 2023 | ISSN: 2215-3411. 112

the modulus of elasticity (MPa) and compressive strength (MPa) of each one of them. A statistically significant difference (p=0.001) was obtained in the printing properties of the biomaterial 88C, compared to 90B and pure PLA and the 88C presented the best 3D printing characteristics. In addition, it also presented the best mechanical properties compared to the other groups of materials. Although the difference between these was not statistically significant (p=0.388), in the structures of the 88C biomaterial, values of compressive strength (8,84692 MPa) and modulus of elasticity (43,23615 MPa) were similar to those of cancellous bone in the jaws could be observed. Because of this result, the 88C biomaterial has the potential to be used in the manufacture of bioscaffolds in tissue engineering.

KEYWORDS: Bio scaffolding; PLA; 3D printing; FDM; Biomaterial; Bone [AND] defect; Diatoms; Calcium phosphate.

RESUMEN: El objetivo es determinar cuál biopolímero presenta las mejores características de impresión 3D y propiedades mecánicas para la fabricación de un bioandamiaje, utilizando la técnica de impresión por deposición fundida, con modelos generados a partir de un archivo en formato STL que se obtuvo de un Micro-CT Scan de una estructura osea de cresta iliaca bovina. Mediante un estudio exploratorio, se realizaron 3 grupos de estudio con trece estructuras impresas de cada uno. El primero, se compone 100% de PLA. El segundo, 90B, se le agrega 1g de extracto de diatomea, y el tercero, 88C, se diferencia del anterior ya que contiene además, 1g de fosfato de calcio. A las 39 estructuras impresas se les realizó una prueba de inspección visual, por lo que se requirió la confección de un patrón de oro en resina, con mayor detalle y similitud a la estructura ósea escaneada. Finalmente, las estructuras fueron sometidas a una fuerza compresiva (N) para la obtención del módulo de elasticidad (MPa) y de la resistencia compresiva (MPa) de cada una de ellas. Se obtuvo una diferencia estadísticamente significativa (p=0,001) en las propiedades de impresión del biomaterial 88C, con respecto al 90B y al PLA puro, presentando las mejores características de impresión 3D. Además, obtuvo las mejores propiedades mecánicas en comparación con los otros grupos de materiales. Aunque la diferencia entre estos no fue estadísticamente significativa (p=0,388), en las estructuras del biomaterial 88C, se pudieron observar valores de resistencia compresiva (8,84692 MPa) y módulo de elasticidad (43,23615 MPa) que son semejantes a los del hueso esponjoso de los maxilares. A razón de este resultado, el biomaterial 88C cuenta con el potencial para ser utilizado en la fabricación de bioandamiajes en la ingeniería tisular.

PALABRAS CLAVE: Bioandamiaje; PLA; Impresión 3D; FDM; Biomaterial; Defecto[AND] óseo; Diatomeas; Fosfato de calcio.

INTRODUCTION

Defects in craniofacial bone tissue come from multiple complications such as trauma, surgical resections, congenital defects (for example cleft lip and palate), pathologies, and frequent chronic infections (e.g. tooth decay and periodontal disease). Given this problem, research has had to be developed in new fields, such as tissue engineering for the manufacture of bone grafts (1,25), which has allowed great advances in regenerative medicine, restoring functionality to bone tissue.

Since the 2000s, 3D printing applications have been made in bone tissue engineering. Scaffolds have been produced to provide support for cells to grow and regenerate before migrating to the site of interest to form new tissue. Another application is the regeneration of bone tissue, by producing scaffolds as temporary structures that induce bone regeneration and subsequently, the material is reabsorbed by osteoclasts (26). Therefore, an ideal scaffold reabsorbs at a rate equal to that of the developing tissue (12,13).

For the development of a scaffold model that reproduces bone morphology, it is possible to implement Micro-CT Scan technology, since it achieves excellent reproducibility and precision of the images obtained by scanning bone tissue in DICOM files, which can then be converted to STL format, which is compatible with 3D printers (3,8).

Fused Deposition Modeling (FDM) is a 3D printing technique consisting of additive fabrication, that can produce 3D objects with complex and precise geometries from CAD data (14, 21,11). This is based on the reproduction of a 3D model from the superposition of sequential layers of a thermoplastic material that has a low melting point. This type of printing uses an XYZ plotter device, an extrusion head, and has a plastic filament that through a heater, passes into a semi-molten state,

to be deposited on a platform, where a structure is formed layer by layer (13,28). The fused deposition modeling method requires thermoplastic materials with suitable physical and mechanical properties, such as polylactic acid (PLA), which is a material that allows the manufacture of complex structures with a good degree of precision (6,7,20). Incorporating other components to PLA seeks to improve the characteristics of a bioscaffold, such as biocompatibility, biodegradability, and mechanical properties similar to bone (27). Among the components that can be added for biomaterial enhancement in the creation of scaffolds for bone regeneration are diatom frustules which, thanks to their silica composition and porous surfaces, when in contact with osteoprogenitor cells increase longevity and cellular osteoactivity (5,9,18,22,23). This generates an optimal environment for the formation of bone tissue with clinical application in maxillary defects such as cleft lip and palate (10,19). Another component that can improve the biomaterial is calcium phosphate, which is chemically similar to human bone and has optimal biodegradability, thus allowing bone growth and regeneration once it has been degraded, as well as activation of the osteogenesis process (16,24).

The objective of this research is to determine which biopolymer presents the best 3D printing characteristics and mechanical properties for the fabrication of a bioscaffold, assuming that there is no statistically significant difference between any of the biomaterials to be observed, in terms of printing characteristics and mechanical properties.

METHODS

An exploratory experimental study was developed, where an open protocol was implemented to be able to print from a Micro-CT Scan the recreation of a bone structure that can be used, in the future, as a bioscaffold and thus, indicate the composition of the biomaterial that has the best printing characteristics to achieve this function.

This project was approved by the Scientific Ethics Committee of the University of Costa Rica, in its 126th session, on November 28, 2018. An N force was applied to each of the printed structures through a mechanical compression test to obtain the modulus of elasticity and compressive strength.

The microtomography is from a bovine iliac crest, taken with a Carl Zeiss Ltd Micro-CT Scan, CT5000, from the School of Engineering Design and Mechanics, University of Portsmouth, United Kingdom. The 3D structures were printed using the fused deposition modeling technique with the Original Prusa 3i printer. Three types of polylactic acid or PLA-based biopolymers were manufactured using the Filabot EX2 filament extruder. The first biopolymer is 100% composed of PLA. The biomaterial 90B, is composed of 20g of polylactic acid per 1g of diatom extract and 88C differs from the previous one as it also contains 1g of calcium phosphate.

A sample was determined with a confidence level of 95%, a goodness of fit of 80%, and a maximum permissible error of 235 MPa in the average compressive strength to be used later in the mechanical tests with the following formula:

$$n \geq \frac{\left(z_{\left(1-\alpha/2\right)} + z_{(1-\beta)}\right)^2}{(d)^2}\sigma^2$$

Where:

- n: sample size
- z(1-α/2): the value associated with the level of confidence in the standard normal distribution.
- z(1-β): the value associated with the power of the test in the standard normal distribution.
- d: the maximum permissible error equal to 5% in MPS strength.
- σ2: maximum variability observed in the study by F.S. Senatovn *et al*.

Once the real values are integrated into the formula, the result is as follows:

$$n = \frac{(1.96+0.84)^2}{(2.35)^2}(9,2)^2 = 13$$

The final sample, according to the described formula, is:

$$n_f = n * c = 3 * 13 = 39$$

Where:

- nf: final sample.
- c: number of interactions in the experiment.

An n of 13 structures was determined for each biopolymer. It was decided to print these structures at a printing scale of 150% since this ratio gave the best printing results.

Failed impressions were taken into account in the collection of results only to indicate the impression feasibility of each group of structures.

A visual inspection test was performed which required the production of a gold standard printed on resinous material, White V4 on the Form 2 printer from Form Labs. The structures that were completely printed were visually evaluated on a scale of I to III, depending on their similarity to the gold pattern printed in resin and according to the following scale (Table 1).

Table 1. The scale of visual inspection of printed structures compared to the resin pattern.

Yes		The impression of the structure is achieved
	I	Closely resembles the resin pattern
	II	Partially resembles the resin pattern
	III	Does not resemble the resin pattern
No		The impression of the structure is not achieved

This visual inspection was carried out by a single operator to ensure the same subjective opinion. Using a digital microscope, photographs of each of the printed structures were obtained and compared with the resin standard created.

Finally, each printed structure was subjected to a compressive force using the Instron Electro Plus E3000 universal testing machine. A compressive force N was applied to each of them, with a displacement of 15mm, at a speed of 5mm/min, to determine the compressive strength and Young's modulus or elasticity of each one of them, to compare the 3 study groups.

Data were stored in Microsoft Excel and analyzed with SPSS version 22 statistical analysis software. Descriptive statistics, including means, standard deviations, and standard errors, were calculated for all measurements.

Once the data for the validation, reliability, and operability of the protocols and results generated were obtained, the distribution of frequencies of the variables, crossing of variables, analysis of statistical association, and analysis of variance was applied as a statistical method; comparisons were made at 95% confidence.

RESULTS

The distribution of the materials according to the printing detail (Table 2) presented a statistically significant difference (p=0.001). As shown in Table 3, the 88C biopolymer presented better printing properties, which can be affirmed because there were more printed structures with good print detail, while with the pure PLA biopolymer, most of the prints had fair print detail and in the 90B biopolymer prints, the print detail was poor.

When looking at the 88C material prints, 80% of them had excellent print detail. To obtain the sample of material 88C, 15 print attempts were made, because 2 of the prints were not completed.

Table 2. Sample distribution according to biomaterial by print detail.

| Material | Print detail | | | | | | Total | |
| | Deficient | | Regular | | Well | | | |
	#	%	#	%	#	%	#	%
88C	2	13,3%	1	6,7%	12	80,0%	15	100%
90B	16	51,6%	4	12,9%	11	35,5%	31	100%
PLA	0	0,0%	12	92,3%	1	7,7%	13	100%
Total	18	30,5%	17	28,8%	24	40,7%	59	100%

Analysis of printing detail of the different types of biopolymers according to a printing scale poor, fair, or good.

Table 3. Observation of structures printed with 88C, 90B, and PLA material.

Observation	88C Cases	90B Cases	PLA Cases
Excellent	12	11	1
Incomplete printing	2	18	
Notches and color changes		2	12
Excess material at the base	1		

The structures of 90B, 88C, and PLA materials are grouped according to their observations when printed.

Biomaterial 90B presented greater variability in the observations, mostly because the impression was not 100% complete. On the other hand, in the PLA biomaterial, only one sample was considered excellent because the majority of them presented areas of material with a color change or with notches. Finally, 86.7% of the total impressions of the 88C biomaterial were able to print 100% in the first attempt. With biomaterial 90B, 58.1% of the structures failed to print 100% on their first attempt; therefore, to complete the sample, a total of 31 attempts were made. However, when using the pure PLA biomaterial, 100% of the impressions were obtained on the first attempt with alterations (Table 4).

The structures of the 88C and 90B materials, which achieved 100% printing, were visually compared with the gold standard printed on White V4 (Figure 1) resin and it was observed that they partially resemble the gold standard, however, the structures of the PLA prints do not resemble the gold standard (Table 5).

When subjecting the bioscaffolds to mechanical strength tests, as shown in Table 6, the force (N) used to obtain the compressive strength (MPa) and modulus of elasticity (MPa) of each of the biomaterials used is detailed. Based on the variables mentioned above, it can be observed that the average of the PLA biomaterial was lower than that of the 90B, while the 88C biomaterial obtained the highest values, with an average force of 1272.2308 N, a compressive strength of 8.84692 MPa and a modulus of elasticity of 43.23615 MPa.

The most variable material among the three, in terms of strength and compressive strength results, was 90B, while 88C was in the variable of the modulus of elasticity.

Since there is no homogeneity of variances among the biomaterials (p=0.0001), we proceeded to use the Jonckheere-Terpstra test to test the hypothesis that the averages of strength (p=0.009) and compressive strength (p=0.014) show no difference between all the groups of biopolymers, while no statistically significant difference (p=0.388) was found between the groups in the modulus of elasticity.

Table 4. Printing attempts according to biomaterial by achievement percentage.

Material	Print				Total	
	Not achieved		Achieved			
	#	%	#	%	#	%
88C	2	13,3%	13	86,7%	15	100,0%
90B	18	58,1%	13	41,9%	31	100,0%
PLA	0	0,0%	13	100,0%	13	100,0%
Total	20	33,9%	39	66,1%	59	100,0%

The percentage of print attempts to obtain 100% of the structure is displayed according to the type of material.
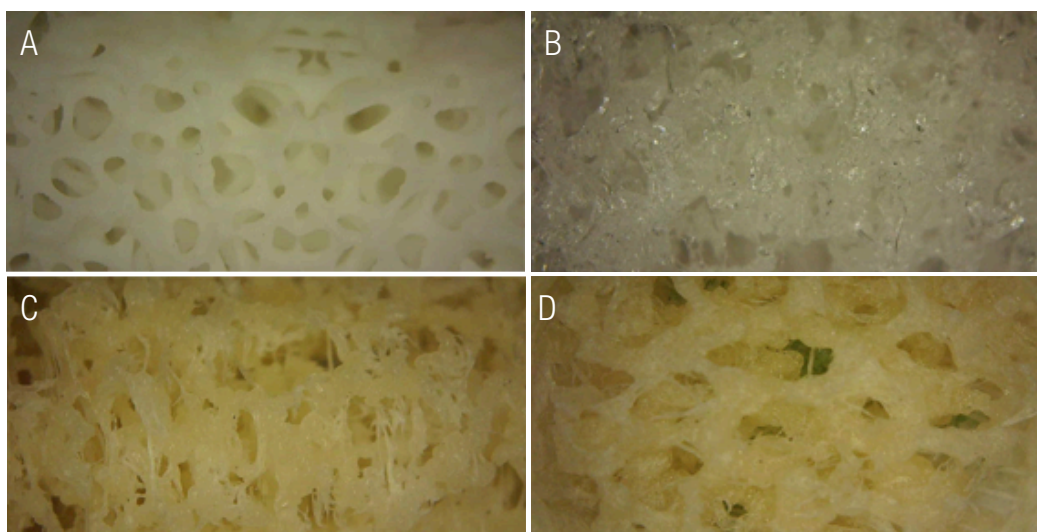
Figure 1. Microscope images at 40 X resolution.
The images show: A. gold standard, B. PLA pure, C. 88C, and D. 90B.

Table 5. Inspection results and visual comparison with the gold standard.

| Material | Visual inspection result | | | | | | | |
| | No resemblance to the gold standard | | Partially resembles the gold standard | | Closely resembles the gold standard | | Total | |
	#	%	#	%	#	%	#	%
88C	0	0,0%	13	100,0%	0	0,0%	13	100,0%
90B	0	0,0%	13	100,0%	0	0,0%	13	100,0%
PLA	13	100,0%	0	0,0%	0	0,0%	13	100,0%
Total	13	33,3%	26	66,7%	0	0,0%	39	100,0%

Table 6. Results of the variables Force (N), Compressive Strength (MPa), and Modulus of Elasticity (MPa), according to the material sample.

Variables	Group	Median	Standard deviation	N
Force (N)	88C	1272,2308	324,83230	13
	90B	463,7454	362,38107	13
	Pure PLA	200,9923	71,32428	13
	Total	645,6562	538,20976	39
Compressive strength (MPa)	88C	8,84692	2,412745	13
	90B	3,50477	2,739083	13
	Pure PLA	1,44308	0,631524	13
	Total	4,59826	3,784662	39
Modulus of elasticity (MPa)	88C	43,23615	39,573622	13
	90B	21,74569	13,045416	13
	Pure PLA	4,21385	2,311495	13
	Total	23,06523	28,484038	39

DISCUSSION

Regarding the results of the PLA biopolymer printing tests, being a pure material, 100% of the prints were obtained in the first attempt. However, most of the samples presented areas with color changes and notches in their structure.

About biomaterial 90B (composed of 95.2% of PLA and 4.8% of diatom frustules), it required the most repetitions of printing attempts of the structures, due to clogging of the printer extruders with the biopolymer.

The biopolymer material 88C (composed of 91% of PLA, 4.5% of diatomaceous frustules, and 4.5% of calcium phosphate), presented a better behavior when printing the structures, with 86.7% of the samples printed 100% on the first try. It also showed the best results in the mechanical tests, obtaining an average force of 1272.2308N, a compressive strength of 8.84692 MPa, and a modulus of elasticity of 43.23615 MPa. The mentioned results of biopolymer 88C were the highest values when compared to the other two materials and it is worth noting that they coincide with the ranges of the mechanical properties of cancellous bone reported in the literature, where the compressive strength is in the range of 2-12 MPa and the values achieved in the modulus of elasticity are close to the range of 50-500 MPa (4).

Upon visual inspection of the impressions and comparison with the gold standard made of resin (technique with better resolution), it was observed that 100% of the structures printed with the 88C and 90B biopolymers partially resemble the gold standard, while the PLA structures do not resemble the gold standard at all.

Regarding the null hypothesis, it must be partially rejected, since a statistically significant difference (p=0.001) was obtained in the printing properties of the 88C biomaterial compared to 90B and pure PLA. Due to its composition based on PLA, diatom frustules, and calcium phosphate, the 88C biopolymer has the best 3D printing characteristics, using the fused deposition modeling technique, from stereolithographic models obtained with Micro-CT Scan. In addition, the 88C biomaterial also showed the best mechanical properties compared to the other groups of materials. Although the difference between them was not statistically significant (p= 0.388), in the 88C biomaterial structures, values similar to those of cancellous bone could be observed.

To create a biopolymer for the manufacture of bioscaffolds, each printing filament used was made by hand, making it difficult to control their diameter.

The Prusament filaments used in the Original Prusa 3i 3D printer, are manufactured with a homogeneous and consistent diameter of approximately 1.75mm (tolerance of ±0.002). According to Cardona *et al.* (2016), inconsistent filament diameter can cause serious complications during extrusion, but it remains debatable whether small deviations in diameter can affect the printing result (17). The above is observed in the impressions of filament 90B, in which 58.1% of impressions failed.

The biomaterial 88C filament presented a better behavior when printing structures, this may be due to its composition: PLA, diatoms, and calcium phosphate. The latter component is a ceramic material, which has been incorporated into different bioscaffolds to improve their mechanical properties, this is evidenced by the values obtained in compressive strength, which is the most commonly tested mechanical property for ceramic scaffolds (16). Calcium phosphate and bone apatite (mineral phase of bone tissue) are similar in both their crystal structure and chemical structure. Apart from improving the mechanical characteristics of the scaffold, it has osteoconductive, osteogenic, and osseointegration properties (16).

Also, by adding diatom frustules to a material such as PLA, a nanostructure (composed of silica) is obtained in the printed bio scaffolding, which was possible using a low-cost, not very specialized 3D printer. This structure would generate a favorable environment for interaction with the cells (osteoactivity) because it has a great potential for osteoinduction and osteoregeneration, since silica plays a fundamental role in bone formation in the body, in the osteoblast function, and the induction of the mineralization process (6,9).

This study is a point of reference for developing research focused on tissue engineering applied to tissue regeneration in bone defects, such as patients with cleft lip and palate, because there are currently very few studies in the literature on tissue regeneration of bone defects associated with this condition, although it is one of the most common craniofacial abnormalities in humans (15). In this way, a bioscaffold 3D printed with optimal mechanical characteristics could be used to replace missing bone tissue in these patients. Thanks to this study it is possible to observe the behavior of a new biomaterial that could be used in the field of tissue engineering for bone regeneration in the future, which is made up of low-cost materials such as diatom extract, calcium phosphate, and the PLA. Taking into account that the 88C group offered the best printing and mechanical test results, it is expected that at some point the manufacturing processes of this filament will be standardized, to have more control over the thickness and other variables, such as diameter, consistency and mechanical properties that may affect the filament manufacturing process.

CONCLUSION

The biomaterial with the best printing characteristics and mechanical properties, to elaborate a bioscaffold using 3D printing using the fused deposition modeling technique from stereolithographic models derived from a Micro-CT Scan, was the 88C biopolymer. The combination of PLA, calcium phosphate and diatom frustules not only provides biocompatibility and biodegradability properties but also provides better compressive strength to the bioscaffolds, and for this reason, it can be said that it presented a mechanical behavior similar to that of the cancellous bone of the maxillae.

The 88C biopolymer could become a material with the potential to be used in the manufacture of bioscaffolds in tissue engineering. Using accessible and affordable 3D printers and materials, the creation of a bioscaffold with good printing characteristics can be achieved.

AUTHOR CONTRIBUTION STATEMENT

ACKNOWLEDGMENTS

REFERENCES

1. Chaudhari A.A., Vig K., Baganizi D.R., Sahu R., Dixit S., Dennis V., et al. Future prospects for scaffolding methods and biomaterials in skin tissue engineering: A review. Int J Mol Sci. 2016 Nov 25; 17 (12): 1974.

2. Murphy W., Black J., Hastings G. Handbook of biomaterial properties. 2nd ed. New York: Springer. 2016.

3. Bose S., Vahabzadeh S., Bandyopadhyay A. Bone tissue engineering using 3D printing. Mater Today (Kidlington). 2013 Dec 01; 16 (12): 496-504.

4. Hutmacher D.W., Schantz J.T., Lam C.X.F., Tan K.C., Lim T.C. State of the art and future directions of scaffold-based bone engineering from a biomaterials perspective. J Tissue Eng Regen Med. 2007 Jul-Aug; 1 (4): 245-260.

5. Amoda A., Borkiewicz L., Rivero-Müller A., Alam P. Sintered nanoporous biosilica diatom frustules as high-efficiency cell-growth and bone-mineralization platforms. Mater Today Commun. 2020 Feb 24; 1-9.

6. Serra T., Mateos-Timoneda M.A., Planell J.A., Navarro M. 3D printed PLA-based scaffolds: a versatile tool in regenerative medicine: A versatile tool in regenerative medicine. Organogenesis. 2013 Oct 1; 9 (4); 239-244.

7. Rodrigues N., Benning M., Ferreira A.M., Dixon L., Dalgarno K. Manufacture and characterization of porous PLA scaffolds. Proceeding CIRP. 2016 Aug 26; 49: 33-8.

8. Orhan K. Micro-computed Tomography (micro-CT) in Medicine and Engineering. 1st ed.New York: Springer. 2020.

9. Maher S., Kumeria T., Aw M.S., Losic D., Martín-del-Campo M., Rosales-Ibañez R., et al. Diatom Silica for Biomedical Applications: Recent Progress and Advances. Advanced Healthcare Materials. 2018 Oct; 7 (19): e1800552 .

10. Martín-del-Campo M., Rosales-Ibañez R., Rojo L. Biomaterials for Cleft Lip and Palate Regeneration. International Journal of Molecular Sciences. 2019 May 02; 20 (9): 2176.

11. Chacón J.M., Caminero M.A., García-Plaza E., Núñez P.J. Additive manufacturing of PLA structures using fused deposition modeling: Effect of process parameters on mechanical properties and their optimal selection. Mater Des. 2017 Jun 15; 124: 143-57.

12. Bakhtiar S.M., Butt H.A., Zeb S., Quddusi D.M., Gul S., Dilshad E. 3D Printing Technologies and Their Applications in Biomedical Science. In: Omics Technologies and Bio-Engineering. Elsevier. 2018; 167-189.

13. Zhang L., Yang G., Johnson B.N., Jia X. Three-dimensional (3D) printed scaffold and material selection for bone repair. Acta Biomater. 2019 Jan 15; 84: 16-33.

14. Gibson I., Rosen D., Mahyar K. Additive Manufacturing technologies. 3rd ed. Atlanta: Springer. 2020.

15. The story behind Prusament [Internet]. Prusament. 2021 [cited 26 October 2021]. Available at: https://prusament.com/es/la-historia-detras-de-prusament/

16. Denry I., Kuhn L.T. Design and characterization of calcium phosphate ceramic scaffolds for bone tissue engineering. Dental Materials. 2016 Jan 32; (1): 43-53.

17. Cardona C., Curdes A., Isaacs A. Effects of filament diameter tolerances in fused filament fabrication. IU. J. Undergrad. 2016 May 31; 2 (1): 44-47.

18. Diab M., Mokari T. Bioinspired Hierarchical Porous Structures for Engineering Advanced Functional Inorganic Materials. Adv Mater. 2018 Oct; 30 (41): e1706349.

19. Brézulier D., Chaigneau L., Jeanne S., Lebullenger R. The Challenge of 3D Bioprinting of Composite Natural Polymers PLA/Bioglass: Trends and Benefits in Cleft Palate Surgery. Biomedicines. Oct 27; 9 (11): 1553.

20. Displer T., Fournier N., et al. Polymer-Bioactive Glass Composite Filaments for 3D Scaffold Manufacturing by Fused Deposition Modeling: Fabrication and Characterization. Front Bioeng Biotechnol. 2020 Jun 24; 8: 55221.

21. Wasti S. Adhikari S. Use of Biomaterials for 3D Printing by Fused Deposition Modeling Technique: A Review. Front Chem. 2020 May 7; 8: 315.

22. Abdelhamid M., Pil Pack S. Biomimetic and Bioinspired Silicifications: Recent Advances for Biomaterial Design and Applications. Acta Biomater. 2021 Jan 15;120: 38-56.

23. Reid A., Buchanan F., et al. A review on diatom biosilicification and their adaptive ability to uptake other metals into their frustules for potential application in bone repair. J Mater Chem B. 2021 Sep 14; 9 (34): 6728-6737.

24. Gjerde C., Mustafa K., et al. Cell therapy induced regeneration of severely atrophied mandibular bone in a clinical trial. Stem Cell Research and Therapy. 2018 Aug 9; 9 (1): 213.

25. Shafiee A., Atala A. Tissue Engineering: Towards a New Era of Medicine. Reviews in advance. Annu Rev Med.2017 Jan; 68: 29-40.

26. Perić Kačarević Z., Rider P., et al. An Introduction to bone tissue engineering, The International Journal of Artificial Organs. 2020 Feb; 43 (2): 69-86.

27. Ghassemi T., Shahroodi A., Ebrahimzadeh M.H., Mousavian A., Movaffagh J., Moradi A. Current concepts in scaffolding for bone tissue engineering. Arch Bone Jt Surg. 2018 Mar; 6 (2): 90-9.

28. César-Juárez A., Olivos-Meza A., Landa-Solís C., Cárdenas-Soria V., Silva-Bermúdez P., Suárez-Ahedo C. et al. Use and application of 3D printing and bioprinting technology in medicine. Rev. Fac. Med. (Mex.). 2018 Dec; 61 (6): 43-51.